Supplement of Geochronology, 2, 133–154, 2020
https://doi.org/10.5194/gchron-2-133-2020-supplement

Supplement of

Seasonal deposition processes and chronology of a varved Holocene lake sediment record from Chatyr Kol lake (Kyrgyz Republic)

Julia Kalanke et al.

Correspondence to: Julia Kalanke (juliak@gfz-potsdam.de)

Supplement

The sediment record from Lake Chatyr Kol was investigated within the framework of the projects CADY (Central Asian Climate Dynamics) and CAHOL (Central Asian Holocene Climate).

Figures

Fig. S1 Correlation of SC17_7 (right) with the top of the composite profile CHAT12 (left): Red lines signify marker layers. Dotted red lines indicate slightly calcitic enriched intervals. Thin sections are displayed next to the composite.

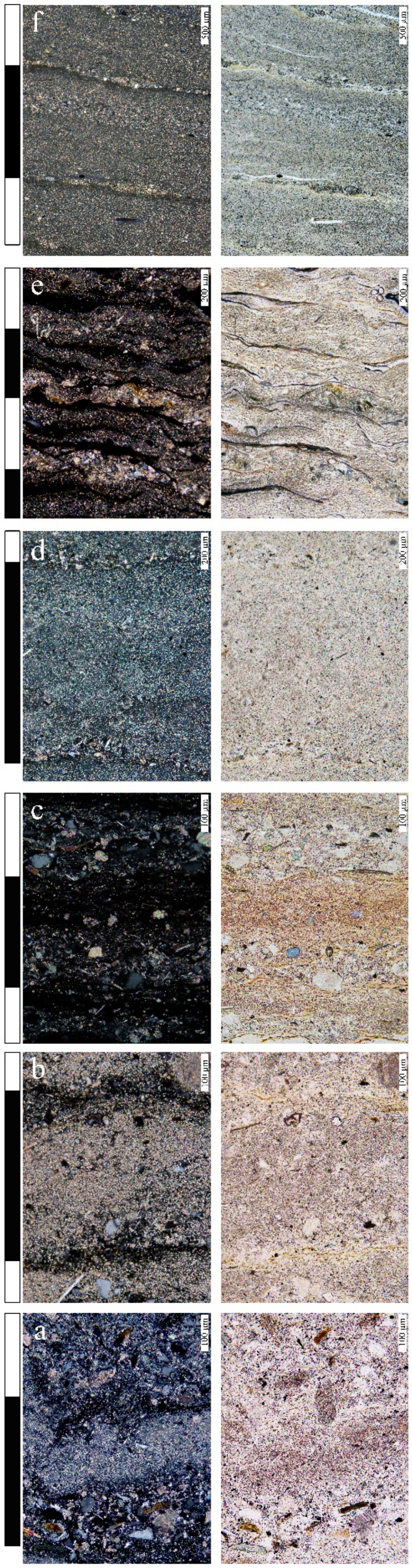

Fig. S2 Microscopic pictures of different microfacies types (chapter 4 and figure 4 in the manuscript): a) clastic-aragonite varves, b) calcitic-clastic varves, c) clastic-diatom varves, d) clastic-calcitic varves, e) organic-clastic varves, f) clastic-organic varves. Each black and white bar (left) indicate one varve. Note the different scales in the upper right corners of each picture.

*Tab. S1 Gamma spectrometry results. count unc. = count uncertainty, * not used for CRS model calculations.*

keV						661.66		46.54		295.24		351.93				
Abundance						0.851		0.0425		0.185		0.358				
Efficiency G1						0.163		0.6056		0.3626		0.3217				
Efficiency G2						0.176		0.6638		0.3942		0.3319				
Composite Depth (cm)	**Depth (cm) Core SC 17-7**	**DD (g/cm³)**	**m (g)**	**Det**	**t_{mess} (d)**	**^{137}Cs (mBq/g)**	**^{137}Cs count unc. (%)**	**^{210}Pb (mBq/g)**	**^{210}Pb count unc. (%)**	**^{214}Pb (mBq/g)**	**^{214}Pb count unc. (%)**	**^{214}Pb (mBq/g)**	**^{214}Pb count unc.(%)**	**$^{210}Pb_{supp}$ (mBq/g)**	**$^{210}Pb_{unsupp}$ (mBq/g)**	**Sample Number**
-1.0	0.25	0.164	1.04366	G1	3.06	53.6	2.6	512.4	2.2	12.2	11.0	15.5	5.5	13.9	498.6	1
-0.5	0.75	0.294	1.12885	G1	3.79	49.3	2.2	424.1	2.1	22.5	5.9	18.8	2.5	20.6	403.5	2
0.0	1.25	0.319	1.06359	G2	3.06	47.3	2.9	264.4	3.4	16.8	8.3	13.0	6.0	14.9	249.5*	3
0.0	1.25	0.319	1.06359	G1	6.99	48.4	1.8	308.1	2.1	13.2	6.0	13.4	4.2	13.3	294.8	4
0.5	1.75	0.207	1.02092	G1	2.70	65.1	2.5	259.7	3.5	20.5	7.8	19.5	5.3	20.0	239.7	5
1.0	2.25	0.156	1.08748	G2	3.17	97.6	1.7	266.2	3.1	25.9	5.9	17.8	5.1	21.8	244.4	6
1.5	2.75	0.138	1.02426	G1	3.85	162.1	1.2	279.6	3.0	25.0	7.8	26.9	4.5	26.0	253.6	7
2.0	3.25	0.135	1.02441	G1	3.14	209.0	1.2	253.4	3.7	27.2	7.4	30.3	4.2	28.7	224.7	8
2.5	3.75	0.147	1.14065	G1	1.98	236.1	1.3	251.8	4.6	34.5	6.9	32.1	4.8	33.3	218.5*	9
2.5	3.75	0.147	1.14065	G2	5.02	236.3	0.8	217.3	2.8	28.8	5.3	30.9	3.3	29.8	187.5	10
3.0	4.25	0.144	1.18116	G2	2.00	266.4	1.2	195.5	5.4	32.2	7.4	26.7	6.1	29.5	166.0	11
3.5	4.75	0.107	1.06028	G2	4.89	302.7	0.7	196.8	3.6	30.6	51.7	33.1	4.0	31.9	165.0	12
4.0	5.25	0.112	1.00751	G1	3.16	295.8	1.0	202.8	4.5	40.5	5.3	36.3	3.7	38.4	164.4*	13
4.0	5.25	0.112	1.00751	G1	4.18	296.3	0.9	215.6	3.5	40.4	4.5	34.6	3.2	37.5	178.1*	14
4.0	5.25	0.112	1.00751	G2	6.73	300.3	0.7	185.5	4.3	33.7	4.7	35.3	3.1	34.5	151.0	15
4.5	5.75	0.132	1.08969	G1	2.94	259.5	1.1	182.8	5.0	32.0	6.4	36.6	3.7	34.3	148.5	16
5.0	6.25	0.146	1.04027	G2	3.17	202.3	1.2	187.6	4.4	36.0	5.9	41.8	3.8	38.9	148.7	17
5.5	6.75	0.137	1.0732	G1	2.98	133.1	1.5	174.8	4.6	38.4	5.5	35.9	3.6	37.1	137.7*	18
5.5	6.75	0.137	1.0732	G2	4.20	136.7	1.2	180.7	5.0	37.0	5.5	35.4	3.5	36.2	144.5	19
6.0	7.25	0.169	0.98522	G1	1.84	93.2	2.5	171.7	6.4	46.8	6.5	32.3	5.2	39.6	132.1*	20
6.0	7.25	0.169	0.98522	G2	3.85	95.8	1.7	154.6	5.1	32.6	6.8	39.7	3.5	36.1	118.5*	21
6.0	7.25	0.169	0.98522	G2	6.99	94.8	1.3	161.8	4.6	41.2	3.9	43.2	2.4	42.2	119.6	22
6.5	7.75	0.140	1.04013	G2	2.95	65.8	2.4	145.7	6.2	41.3	4.9	40.4	3.3	40.9	104.9*	23
6.5	7.75	0.140	1.04013	G1	4.90	62.3	1.9	151.7	4.4	42.4	3.8	37.8	2.8	40.1	111.6	24
7.0	8.25	0.132	0.97056	G2	2.97	51.8	2.9	134.0	7.1	45.7	5.5	39.1	3.8	42.4	91.6*	25
7.0	8.25	0.132	0.97056	G1	3.15	48.9	2.7	135.1	5.6	45.8	4.8	38.8	3.5	42.3	92.8	26

Composite Depth (cm)	Depth (cm) Core SC 17-7	DD (g/cm³)	m (g)	Det	t_{mess} (d)	^{137}Cs (mBq/g)	^{137}Cs count unc. (%)	^{210}Pb (mBq/g)	^{210}Pb count unc. (%)	^{214}Pb (mBq/g)	^{214}Pb count unc. (%)	^{214}Pb (mBq/g)	^{214}Pb count unc.(%)	$^{210}Pb_{supp}$ (mBq/g)	$^{210}Pb_{unsupp}$ (mBq/g)	Sample Number
7.5	8.75	0.168	1.13756	G2	2.71	41.7	2.9	124.6	5.7	38.9	6.0	41.9	3.5	40.4	84.2*	27
7.5	8.75	0.168	1.13756	G1	2.91	38.9	3.0	134.6	6.2	39.1	4.9	37.2	3.3	38.1	96.5	28
8.0	9.25	0.148	1.15022	G2	2.99	26.6	3.7	89.1	8.0	36.9	5.2	40.4	3.1	38.6	65.5	29
8.5	9.75	0.116	1.07792	G1	2.16	16.9	6.4	95.0	10.0	46.1	5.4	41.8	4.0	43.9	51.5	30
9.0	10.25	0.138	1.04675	G1	4.08	12.5	6.2	97.0	8.6	44.6	4.6	37.4	3.3	41.0	56.1*	31
9.0	10.25	0.138	1.04675	G1	6.73	14.3	4.8	88.4	6.0	42.1	3.6	40.8	2.7	41.5	46.9	32
9.5	10.75	0.106	1.06813	G2	2.16	10.8	8.1	84.3	9.9	34.9	7.1	39.2	3.9	37.1	47.2	33
10.0	11.25	0.131	0.9888	G1	3.98	9.7	9.1	79.9	7.9	43.1	7.9	38.2	3.4	40.7	39.3	34
10.0	11.25	0.131	0.9888	G1	3.81	7.1	12.0	75.5	8.1	37.2	8.1	39.2	3.0	38.2	37.3*	35
10.5	11.75	0.156	1.18173	G2	2.91	7.0	11.2	72.0	8.4	39.0	8.4	38.0	3.4	38.5	33.5	36
11.0	12.25	0.168	1.08336	G2	4.09	4.2	15.7	63.8	8.0	36.7	8.0	39.8	3.1	38.2	25.6	37
11.5	12.75	0.146	1.14027	G1	3.95	4.5	14.6	68.4	9.0	38.9	9.0	37.5	2.9	38.2	30.2	38
12.0	13.25	0.183	0.95955	G1	2.88	3.7	26.9	64.0	11.0	46.8	11.0	41.1	4.0	44.0	20.0	39
12.5	13.75	0.154	1.28248	G1	3.78	3.7	16.4	69.2	9.6	39.5	9.6	39.3	2.7	39.4	29.7	40
13.0	14.25	0.154	0.98268	G2	7.93	3.2	17.9	49.6	7.7	41.7	7.7	46.4	2.1	44.1	5.5	41
13.5	14.75	0.112	1.09286	G2	2.99	3.3	16.5	51.9	11.9	40.8	11.9	37.7	3.4	39.3	12.6	42

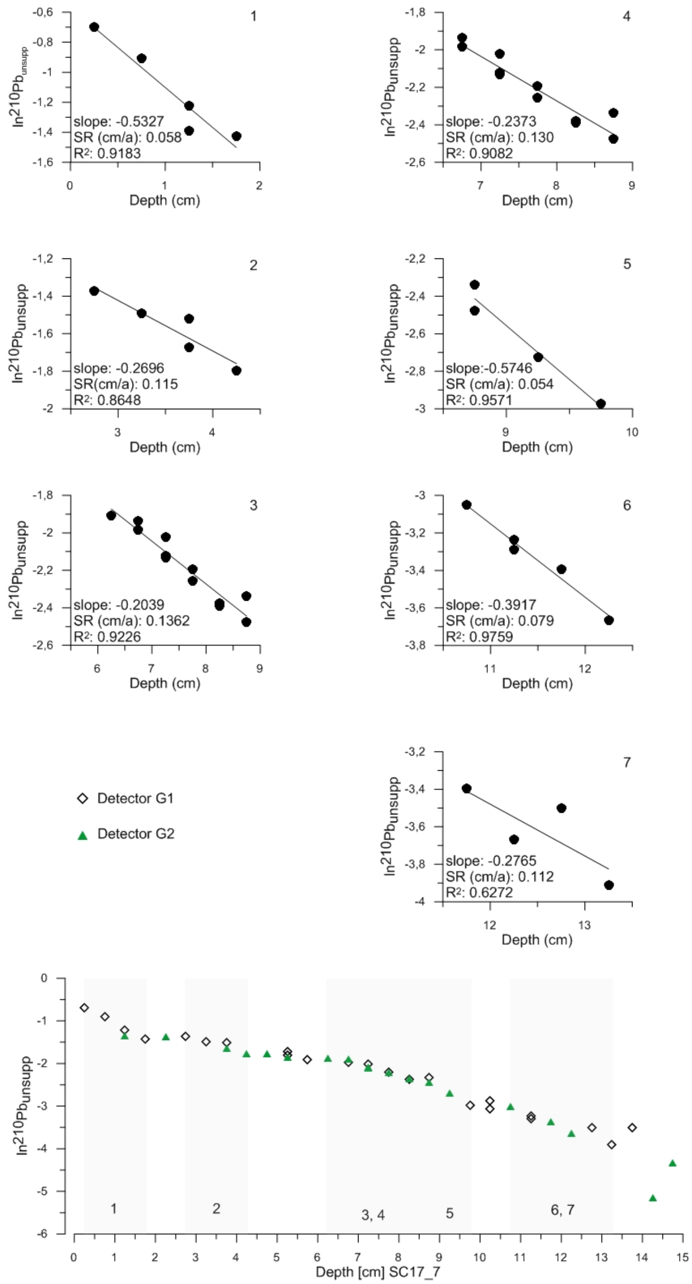

Fig. S3 $\ln^{210}Pb_{unsupp}$ vs depth plot and depth sequences used to calculated sedimentation rates for the CIC model. Light grey bars indicate the used sequences. White square= Detector G1, green triangles= Detector G2.

Tab. S2 Age determination by used depth sequences of $\ln^{210}Pb_{unsupp.}$ The CIC model assumes equal initial concentrations of $^{210}Pb_{unsupp}$ in the sediment regardless of the mass flux at the coring site (c.f. Appleby, 2002). Intercalated sediment sections showed nearly uncorrelated $\ln(^{210}Pb_{unsupp})$ vs. depth relationships between 10.25-9.25, 6.25-4.25, 2.25-1.75 cm depth (Suppl. Fig. 2). Therefore, the initial $^{210}Pb_{unsupp}$ activities of samples that bridged these sections were additionally used to determine time intervals between these samples (italic sequences). We further constrained the CIC model to the ^{137}Cs peak at 5.25 cm depth, located within an uncorrelated $\ln(^{210}Pb_{unsupp})$ vs. depth section between 6.25-4.25 cm depth, assuming it represents the AD 1963 peak of atmospheric nuclear weapon tests.

Marker/ Depth (cm)	**Age Marker**	**Seq. No.**	**from**	**to**	**delta _x (cm)**	**slope**	**SR (cm/a)**	**delta t (a)**	**R^2**	**Dated depths in SC17_7**	Comment
0.25	**2015**										Assumed rel. to top = 2017
1.75	-	1	0.25	1.75	1.5	-0.5327	0.0583	25.7±0.5	0.9183	1.75=1989.3	Calc rel to top (2015-25.7 a)
2.25	-	-	*0.25*	*2.25*	2	-	0.0872	*22.9±0.4*	-	2.25=1992.1	calc rel Top (2015-22,9)
5.25 – ^{137}Cs peak	**1963 ?**										Assuming that ^{137}Cs peak = AD 1963

2.25	-	-	2.25	4.25	2	-0.1943	0.1600	12.5±0.9	0.7793	2.25=1976,1	Cal rel to 4.25=1963.6
2.75	-	2	2.75	4.25	1.5	-0.2696	0.1153	13.0±0.9	0.8648	2.75=1976.6	Cal rel to 4.25=1963.6
2.75	-	-	2.75	4.25	1.5	-0.2094	0.107	14±0.6	0.9933	2.75=1977.6	Cal rel to 4.25=1963.6 (without Nr 9)
3.25	-	-	*3.25*	*5.25*	*2*	-	*0.1989*	*10.1±1.4*	-	*3.25=1973,1*	Cal rel to 4.25=1963.6
4.25	-	-	4.25	5.25	1	-0.0098	3.1717	0.6±0.5	0,978	*4.25=1963.6*	Cal rel to 5.25=1963, ~flat sequence
4.25	-	-	4.25	5.25	*1*	-	*3.1647*	*0.3±0.4*	-	*4.25=1963.3*	Cal rel to 5.25=1963, ~flat sequence
5.75	-	-	4.25	5.75	1.5	-0.0677	0.4591	3.3±0.05	0.6723	*5.75=1960.3*	without Nr 14 & 15
5.75	-	-	*5.25*	*5.75*	*0.5*	-	0.1527	*3.3±0.2*	-	*5.75=1959,7*	*Cal rel to 5.25=1963*
5.75	-	-	5.75	8.75	3	-0.2093	0.1485	20.2±1.2	0.9038	8.75=1939.5	Cal rel to 5.75=1959.7
6.25	-	-	5.25	6.25	1	-	0.3098	3.2±0.1	-	6.25= 1958.1	*Cal rel to 5.75=1959.7*
8.75	-	3	6.25	8.75	2.5	-0.2282	0.1362	18.4±1.2	0.9226	8.75= 1939.7	6.25= 1958.1
8.25	-	-	*5.75*	*8.25*	*3.0*	-	*0.1958*	*15.3±1.13*	-	*8.25=1944,4*	*Cal rel to 5.75=1959.7*
8.75	-	-	5.25	8.75	3.5	-	*0.1817*	*17.1±1.0*	-	8.75=1945.9	Only 5.25 (G1;$^{210}Pb_{unsupp}$=164.4 mBq/g) and 8,75 (G1)
8.75 – Onset ^{137}Cs increase	1945									8.75=1945.9	
7.25	-	-	*7.25*	*8.75*	*1.5*	-	*0.1495*	*10±0.7*	-	*7.25=1955.9*	*Cal. rel. to 8.75=1945.9*
9.75	-	5	8.75	9.75	1	-0.5746	0.0541	18.5±3.4	0.9571	*9.75=1927.4*	Slope change at 8.75, cal. rel. to 8.75=1945.9
10.75	-	-	*8.75*	*10.75*	*2*	-	*0.0963*	*20.8±3.6*	-	*10.75=1925.1*	~flat seq. between 9.75 and 10.25
11.75	-	-	*8.75*	*11.75*	*3*	-	*0.0942*	*31.9±3.8*	-	*11.75 = 1914*	~flat seq. between 9.75 and 10.25
12.25	-	6	10.75	12.25	1.5	-0.3917	0.0794	18.9±1.8	0.9759	12.25 = 1906.2	cal. rel. to 10.75=1925.1.
13.25	-	7	11.75	13.25	1.5	-0.2765	0.1124	13.3±4.4	0.6272	13.25=1900.7	cal. rel. to 11.75=1914
13.25	-	-	*12.25*	*13.25*	*1*	-	*0.1267*	*7.9±4.3*	-	*13.25 = 1898.3*	*cal. rel. to 12.25=1906.2*
13.75	-	-	*12.25*	*13.75*	-	-	*0.3093*	*4.8±0.3*	-	*13.75=1901.4*	*cal. rel.to 12.25=1906.2*
14.75	-	-	*12.25*	*14.75*	*2.5*	-	*0.1103*	*22.7±13.9*	-	*14.75 = 1883.5*	*cal. rel.to 12.25=1906.2*

Tab. S3) Comparison of CIC and CRS model chronologies, calculated sedimentation rates (cm/a) and mass acc. rates ($g/cm^2/a$). Data based on Suppl. Tab. 1 & 2.

Depth SC17_7 (cm)	Composite depth (cm)	*CIC-Model Age	SR (cm/a) CIC Model	*CRS-Model age	SR (cm/a) CRS Model	mass acc. rate ($g/cm^2/a$)
0.25	-1.0	2015	0.06	2015	0.14	0.022
0.75	-0.5	-	0.06	2010	0.08	0.024
1.25	0.0	-	0.06	2004	0.09	0.027
1.75	0.5	1989.3	0.06	1999	0.13	0.027
2.25	1.0	1976.1	0.16	1996	0.15	0.024
2.75	1.5	1976.6	0.12	1993	0.15	0.020
3.25	2.0	1973.1	0.12	1989	0.15	0.021
3.75	2.5	-	0.12	1986	0.15	0.022
4.25	3.0	-	0.12	1983	0.16	0.023
4.75	3.5	-	-	1980	0.19	0.020
5.25	4.0	1963	-	1977	0.18	0.021
5.75	4.5	1959.7	0.15	1974	0.15	0.019
6.25	5.0	-	0.15	1970	0.12	0.017
6.75	5.5	1961.2	0.13	1966	0.11	0.015
7.25	6.0	1955.9	0.13	1961	0.09	0.016
7.75	6.5	-	0.13	1956	0.10	0.014
8.25	7.0	-	0.13	1951	0.11	0.014
8.75	7.5	1945.9	0.13	1945	0.07	0.012
9.25	8.0	-	0.05	1939	0.09	0.013
9.75	8.5	1927.4	0.05	1934	0.12	0.014
10.25	9.0	-	-	1929	0.10	0.014
10.75	9.5	1925.1	0.08	1924	0.11	0.011
11.25	10.0	-	0.08	1919	0.09	0.012
11.75	10.5	1914	0.08	1913	0.07	0.011
12.25	11.0	1906.2	0.08	1906	0.07	0.012
12.75	11.5	-	0.11	1898	0.05	0.008
13.25	12.0	1900.7	0.11	1887	0.04	0.008
13.75	12.5	-	-	1871	0.02	0.004
14.25	13.0	-	-	1854	0.04	0.006
14.75	13.5	1883.5	-	1832	0.02	0.002